JOURNAL OF SPACECRAFT AND ROCKETS
Vol. 38, No. 3, May–June 2001

Entry Dispersion Analysis for the Genesis Sample Return Capsule

Prasun N. Desai* and F. McNeil Cheatwood†
NASA Langley Research Center, Hampton, Virginia 23681-0001

Genesis will be the first mission to return samples from beyond the Earth–moon system. The spacecraft will be inserted into a halo orbit about the sun–Earth collinear libration point L_1 located between the sun and Earth, where it will remain for 2 years collecting solar wind particles. Upon Earth return, the sample return capsule, which is passively controlled, will descend under parachute to Utah. Analysis of the entry, descent, and landing scenario of the returning sample capsule is described. In particular, the use of gyroscopic stiffness to suppress aerodynamic instabilities is presented. The robustness of the overall entry sequence is assessed through a Monte Carlo dispersion analysis, where the impact of off-nominal conditions is ascertained. The dispersion results indicate that the capsule attitude excursions near peak heating and drogue chute deployment are within Genesis mission limits. Additionally, the size of the resulting 3-σ landing ellipse is 47.8 km in downrange by 15.2 km in crossrange, which is within the Utah Test and Training Range boundaries.

Introduction

THE fifth of NASA's *Discovery*-class missions is a sample return mission known as Genesis. The spacecraft will be inserted into a halo orbit about the sun-Earth collinear libration point L_1 located between the sun and Earth, where it will remain for 2 years collecting solar wind particles (Fig. 1). In Ref. 1, a description of the trajectory design is given. Genesis is scheduled to be launched in August 2001 and will be the first mission to return samples from beyond the Earth–moon system. Upon Earth return in September 2004, the entry capsule (Fig. 2), containing the solar wind samples, will be released from the main spacecraft (decelerating with the aid of a parachute) for a midair recovery in Utah over the U.S. Air Force's Utah Test and Training Range (UTTR). Because of the similarities between the Genesis and Stardust[2] missions (i.e., returning a sample capsule to Earth, decelerating with the aid of a parachute, and landing at UTTR), the Genesis entry builds on the Stardust entry, descent, and landing scenario.[3,4] As with the Stardust mission, approximately 4 h before entry, the sample return capsule (SRC) will be spun up to 16 rpm and separated from the main spacecraft. The SRC has no active control system, and so the spinup is required to maintain its entry attitude (nominal 0-deg angle of attack) during coast. Throughout the atmospheric entry, the passive SRC will rely solely on aerodynamic stability for performing a controlled descent through all aerodynamic flight regimes: hypersonic rarefied, hypersonic transitional, hypersonic continuum, supersonic, transonic, and subsonic. The SRC must possess sufficient aerodynamic stability to overcome the gyroscopic (spin) stiffness to minimize any angle-of-attack excursions during the severe heating environment. Additionally, this stability must persist through the transonic and subsonic regimes to maintain a controlled attitude at parachute deployment.

This paper analyzes the entry, descent, and landing sequence for the returning sample capsule. The analysis is performed through a trajectory simulation of the entire entry (from spacecraft separation to landing) to predict the descent attitude and landing conditions. In addition, a Monte Carlo dispersion analysis is performed to ascertain the impact of off-nominal conditions that may arise during the entry to determine the robustness of the Genesis SRC design. Specifically, the SRC attitude near peak heating and parachute deployment is of interest, along with the landing footprint ellipse. Note that the landing footprint is of interest rather than the footprint at the midair recovery conditions due to range safety requirements for ensuring that the SRC will land within the boundaries of UTTR in the event of air-snatch failure.

Presented as Paper 99-469 at the AAS/AIAA Astrodynamics Specialist Conference, Girdwood, AK, 16–19 August 1999; received 7 June 2000; revision received 28 December 2000; accepted for publication 8 January 2001.

*Aerospace Engineer, Aerospace Systems, Concepts and Analysis Competency; p.n.desai@larc.nasa.gov. Senior Member AIAA.

†Aerospace Engineer, Aerospace Systems, Concepts and Analysis Competency; f.m.cheatwood@larc.nasa.gov.

Analysis

Aerodynamics

An aerodynamic database is one of the models required for the flight dynamics simulation. Because of the similarity of the Genesis and Stardust entry capsules (spherically blunted 60-deg sphere cone forebodies), the Stardust aerodynamic database can serve as the foundation for the Genesis aerodynamic database. That aerodynamic database is constructed from a combination of simple relations such as impact methods and bridging functions, high-fidelity numerical solutions, and ground-based experimental data. The aerodynamic characteristics of the Stardust capsule are described in detail by Mitcheltree et al.[5] and are summarized briefly in the following discussion.

The entry trajectories of Stardust and Genesis traverse many different flow regimes (hypersonic rarefied, hypersonic transitional, hypersonic continuum, supersonic, transonic, and subsonic). Therefore, the aerodynamic database is constructed from a variety of sources. At the outer reaches of the atmosphere, free molecular flow calculations describe the rarefied aerodynamics. In the transitional flow regime, direct simulation Monte Carlo (DSMC) solutions are used to anchor simple bridging functions for the aerodynamic coefficients. In the hypersonic-continuum regime, modified-Newtonian values, anchored with solutions from the computational fluid dynamics (CFD) code LAURA[6] describe the aerodynamics. At supersonic and transonic speeds, the aerodynamics are based on two sets of existing wind-tunnel data. Subsonic aerodynamics are defined by a combination of static wind-tunnel measurements and dynamic free-flight measurements.[7] These sources are blended to form a cohesive database that describes the aerodynamics of the SRC for the expected flight conditions. Figure 3 shows the range of application of the various aerodynamic sources mentioned earlier.

Whereas the Stardust and Genesis SRC forebodies are similar, their afterbodies are quite different. Stardust has a 30-deg truncated cone for its afterbody. Genesis, on the other hand, has a biconic afterbody, whose first cone has a turning angle of 20 deg. As a result, the Stardust aerodynamics database is updated (where appropriate) to reflect these differences.

At hypersonic speeds, the vehicles should have virtually the same aerodynamics characteristics for angles of attack less than 20 deg. Because angles of attack in excess of this level may occur early in the entry trajectory, the free molecular values for Stardust are replaced with results for the Genesis SRC. In the transitional flow regime, several DSMC solutions were performed to confirm that the bridging function tailored to the Stardust entry is appropriate for Genesis

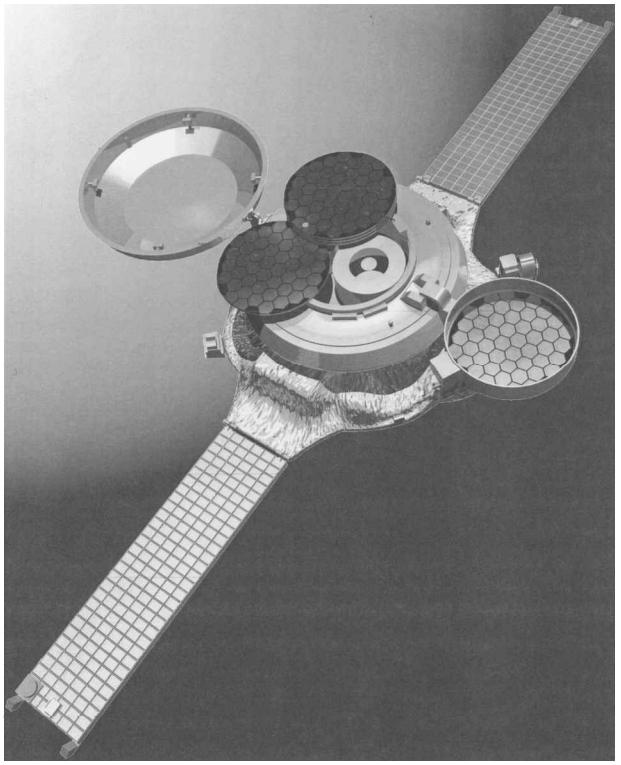

Fig. 1 Genesis spacecraft sampling configuration.

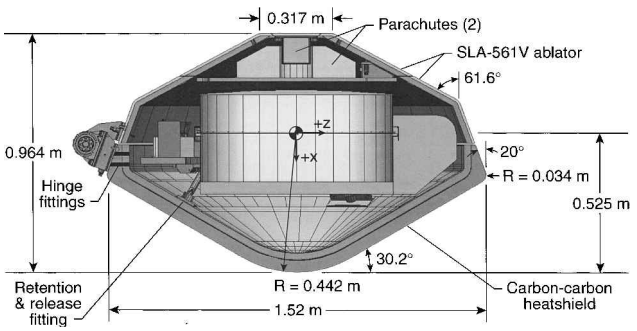

Fig. 2 Genesis SRC configuration.

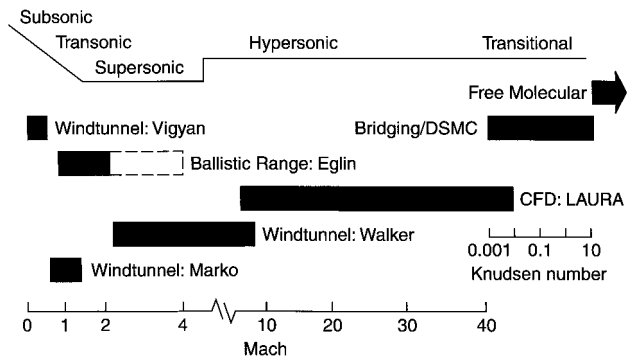

Fig. 3 Genesis SRC aerodynamic database.

as well. For the hypersonic-continuum portion of the entry, the SRC angle of attack will be small, and the Stardust database should again be applicable to Genesis. Examination of CFD solutions verifies that the Stardust database does indeed accurately describe the aerodynamic behavior of the Genesis SRC in this regime. As a result, an update to the aerodynamics in the hypersonic flight regime is not necessary.

As mentioned, for supersonic, transonic, and subsonic speeds, the Stardust static aerodynamics are based on existing wind-tunnel data. These same values are used for Genesis, and the uncertainties placed on the aerodynamics reflect that the afterbodies are different. The Genesis SRC supersonic and transonic aerodynamics are being further characterized using ballistic range tests, which are presently being conducted. When analysis of these test results is completed, the aerodynamic database will be updated (as noted by dashed region in Fig. 3).

Trajectory Simulation

The trajectory analysis is performed using the six- and three-degree-of-freedom (DOF) versions of POST.[8] This program has been utilized previously for similar applications.[9–11] The three-DOF program (which integrates the translation equations of motion) is used from spacecraft separation to atmospheric interface. The six-DOF version of POST (which integrates the translational and rotational equations of motion) is used from atmospheric interface to parachute deployment. The three-DOF program is used again from parachute deployment to landing. The trajectory simulation includes Earth atmospheric (GRAM-95)[12] and gravitational models, capsule separation and noninstantaneous parachute deployment models, as well as capsule aerodynamics and mass properties. The validity of the present approach has been demonstrated recently through comparisons between the Mars Pathfinder preflight predictions of the flight dynamics and the actual flight data.[13]

During the entry, off-nominal conditions may arise that affect the descent profile. These off-nominal conditions can originate from numerous sources: 1) capsule mass property measurement uncertainties, 2) separation attitude and attitude rate uncertainties, 3) limited knowledge of the flight-day atmospheric properties (density, pressure, and winds), 4) computational uncertainty with the aerodynamic analysis, and 5) uncertainties with parachute deployment. In this analysis, an attempt is made to quantify conservatively and model the degree of uncertainty in each mission parameter. For this mission, 47 potential uncertainties were identified. These uncertainties are grouped into two categories: exoatmospheric and atmospheric. Tables 1 and 2 list these uncertainties, respectively, along with the corresponding 3-σ variances. For most of the parameters, a Gaussian distribution is sampled. However, for the radial center-of-gravity (c.g.) offset quadrant and parachute deployment parameters (gravity switch, timers, and dynamic stability aerodynamics), uniform distributions are utilized to model their operating performance.

Note that, although the dispersions in the mass and major moments of inertia of the capsule will be much smaller as launch approaches, large variances are presently used to account for potential variations in the SRC design. Additionally, the dispersion in the SRC separation from the main spacecraft is split into two sources:

Table 1 Exoatmospheric mission uncertainties

Uncertainty	3-σ Variance
Mass properties	
Mass	±1.0 kg
C.G. position along spin axis	±0.0254 cm
C.G. position off spin axis[a]	±0.0254 cm
Major moment of inertia (I_{xx}, I_{yy}, I_{zz})	±10%, 20%, 20%
Cross products of inertia (I_{xy}, I_{xz}, I_{yz})	±0.11 kg-m^2, ±1.1 kg-m^2, ±0.1 kg-m^2
Separation state vector	
Position, Velocity: correlated with covariance matrix producing a $\Delta\gamma_i = \pm 0.06$ deg	
Pitch/yaw attitude	±2.69 deg
Pitch/yaw rate	±4.24 deg/s
Roll rate	±1 rpm
Separation spring-induced velocity	
Body x-axis velocity	±0.0305 m/s
Body y-axis velocity	±0.0203 m/s
Body z-axis velocity	±0.0203 m/s
Precession induced velocity	
Body x-axis velocity	±0.049 m/s
Body y-axis velocity	±0.014 m/s
Body z-axis velocity	±0.014 m/s

[a]Uncertainty sampled using uniform distribution.

Table 2 Atmospheric mission uncertainties

Uncertainty	3-σ Variance
Aerodynamic	
Free molecular aerodynamics	
C_A	±10%
C_N, C_Y	±8%
C_m, C_n	±12%
Hypersonic continuum aerodynamics	
C_A	±4%
C_N, C_Y	±8%
C_m, C_n	±10%
Supersonic continuum aerodynamics	
C_A	±10%
C_N, C_Y	±5%
C_m, C_n	±8%
Subsonic continuum aerodynamics C_A	±5%
Hypersonic dynamic stability coefficients C_{mq}, C_{nr}[a]	±0.28
Supersonic dynamic stability coefficients C_{mq}, C_{nr}[a]	±0.2
Atmosphere	
Pressure, density, winds: GRAM-95 model	3-σ Scale factor
Other	
Drogue chute g switch[a]	±10%
Drogue chute deployment timer[a]	±0.05 s
Drogue chute aerodynamics, C_A[a]	±10%
Main chute deployment timer[a]	±0.05 s
Main chute aerodynamics, C_A[a]	±10%

[a] Uncertainty sampled using uniform distribution.

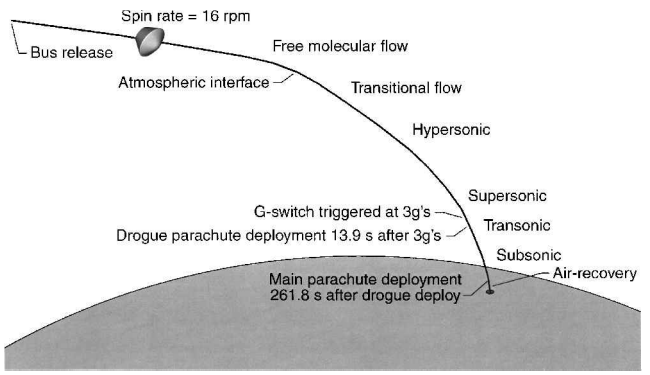

Fig. 4 Nominal Genesis SRC entry sequence.

1) uncertainties during the capsule separation process itself and 2) uncertainties arising from the spacecraft propulsive attitude maneuver that positions the SRC to the proper orientation for release.

Results and Discussion

Nominal Mission

As was the case for the Stardust capsule, the Genesis SRC is aerodynamically unstable in the hypersonic-rarefied and supersonic flight regimes due to the capsule's rearward c.g. location. This aft c.g. location produces a static instability in the free molecular regime, whereas near transonic speeds, a dynamic instability exists. In Refs. 5, 7, and 14, these aerodynamic instabilities are discussed in greater detail. If these instabilities are not addressed, large angle-of-attack excursions could result during the entry. To mitigate the effects of these instabilities, the Genesis entry sequence relies on the Stardust entry, descent, and landing scenario that was developed to traverse successfully all flight regimes. Figure 4 shows the entry sequence, with the terminal descent phase highlighted. An in-depth description is given in Refs. 3 and 4 on the development of the entry scenario utilizing the high entry spin rate, as well as the use of a supersonic drogue parachute deployment.

Upon Earth entry, the entry profile utilizes a g switch, that is, gravity switch, and two timers for deployment of the drogue and main parachutes. The g switch is triggered after sensing 3 g. At that point, the drogue timer is initiated. After 13.9 s, the drogue chute is deployed (approximately Mach 1.4), and the main timer is initiated. At 261.8 s after drogue deploy (approximately at 6 km), the main parachute is deployed. The entry scenario calls for an air snatch of the SRC at an altitude of approximately 2.5 km. These event times are based on the nominal SRC mass properties given in Table 3. This nominal entry sequence is sufficiently robust to accommodate off-nominal conditions during the descent (as confirmed by the Monte Carlo analysis presented in a later section).

Table 3 Nominal mass properties of the SRC

Property	Value
Mass, kg	225
C.G., m	
Along spin axis (x direction, from nose)	0.525
Off spin axis (y direction)	0.0011
Off spin axis (z direction)	0.0022
I_{xx}, kg-m^2 (spin axis)	46.7
I_{yy}, kg-m^2	31.7
I_{zz}, kg-m^2	33.5
I_{xy}, kg-m^2	0.0
I_{xz}, kg-m^2	0.0
I_{yz}, kg-m^2	0.0

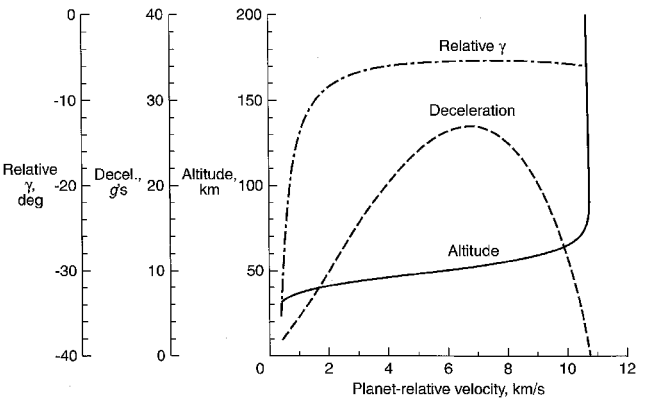

Fig. 5 Nominal entry profile.

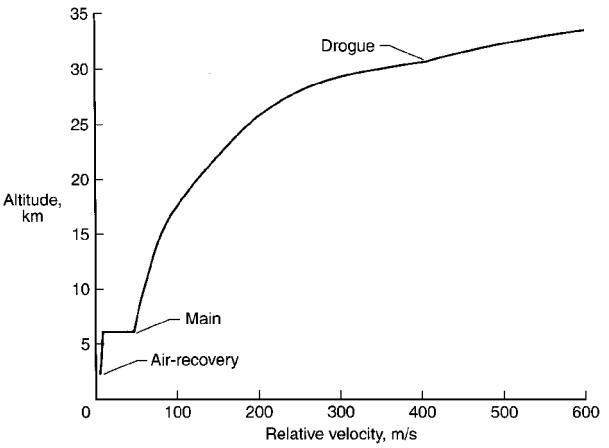

Fig. 6 Nominal entry parachute-deployment profile.

The flight characteristics of the nominal entry are shown in Figs. 5–7. The planet-relative entry flight-path angle γ_r and velocity (referenced to a radius of 6503.14 km) are −8.25 deg and 10.7 km/s, respectively. The maximum deceleration experienced by the SRC during the descent is 26.9 g. Beginning at Mach 1.4 (approximately 30-km altitude), the terminal descent phase of the entry begins. Figure 6 shows the nominal altitudes of the drogue and main parachute deployments.

Similar to the Stardust entry, the Genesis SRC is spun up to 16 rpm and released from the main spacecraft. Unlike Stardust, the high spin rate of the Genesis SRC, coupled with its larger moments of inertia, provide sufficient gyroscopic stiffness to allow the capsule to traverse the hypersonic-rarefied flight regime without experiencing large angles of attack in the transitional flow regime. As seen in

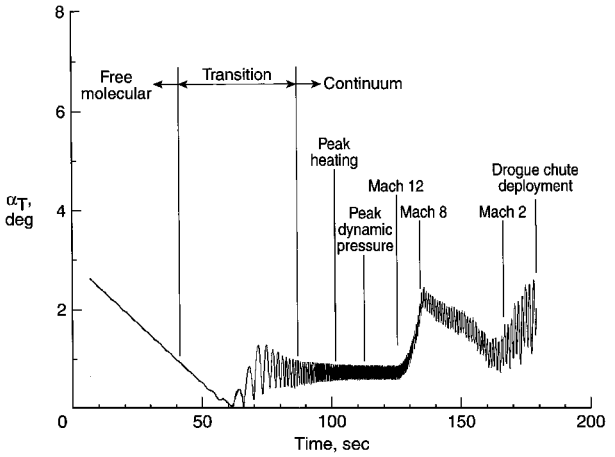

Fig. 7 Nominal Genesis SRC attitude profile.

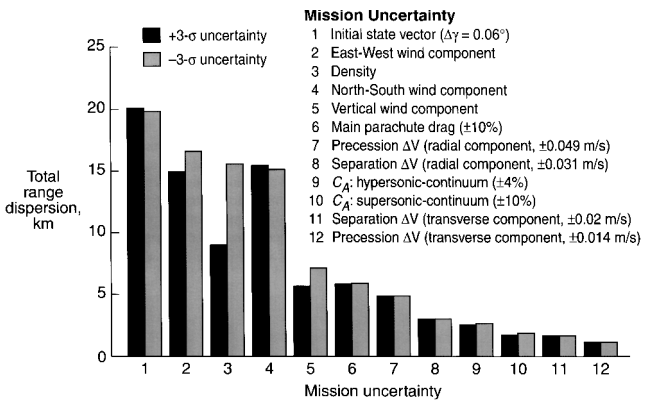

Fig. 8 Major contributors to the total range dispersion (3-σ variance shown in parenthesis).

Fig. 7, the attitude of the capsule in the transitional flow regime does not exceed 1 deg (compared to 7 deg for Stardust). The total angle of attack α_T, which is the included angle between the capsule spin axis and the atmospheric-relative velocity vector, is observed to oscillate about a mean value of 0.8 deg near peak heating (which occurs around Mach 30). As the SRC descends, the static margin decreases near Mach 12 producing a new trim angle of attack because the capsule has a nonzero radial c.g. off set from the spin axis. Consequently, an increase in α_T, from a mean value of 0.8 deg near Mach 12 to a mean value of 1.2 deg near Mach 2, is observed. In transitioning to a new trim point, attitude rates induce an overshoot in α_T (peaking around Mach 8) before receding around Mach 2. As the SRC approaches transonic speeds, the dynamic instability (which is inherent to blunt bodies such as the present capsule configuration) produces an increase in mean α_T until drogue chute deployment (Refs. 3, 4, and 7 describe the impact of this dynamic instability in greater detail).

Monte Carlo Dispersion Analysis

Independent Uncertainty Effects

Before a combination of off-nominal conditions are examined, a sensitivity analysis is first performed to identify the mission uncertainties that have the greatest impact on the overall landing footprint. Each of the 47 mission uncertainties are independently set at their respective ± 3-σ (maximum/minimum) variances. Figure 8 shows the resulting total downrange obtained from the largest contributors to the overall landing footprint. The top four contributors, containing uncertainties in initial state vector and atmospheric wind and density, contribute on the order of 15–20 km each to the landing footprint size. The remaining uncertainties (containing dispersions in spacecraft separation velocity, capsule and parachute aerodynamic drag) produce downrange dispersions of approximately 1–5 km each. Those mission uncertainties that are not depicted lead to downrange dispersions less than 0.5 km.

Multiple Uncertainty Effects

To determine the robustness of the Genesis SRC entry profile, off-nominal conditions are simulated to address uncertainties that may arise during the descent. The impact of multiple uncertainties occurring simultaneously is ascertained by performing a Monte Carlo dispersion analysis. To assure proper Gaussian or uniform distributions for the 47 mission uncertainties identified, 3000 random, off-nominal trajectories are simulated.

The statistical results from the 3000 Monte Carlo simulations are shown in Figs. 9–16. Figures 9–11 show the distribution of the total

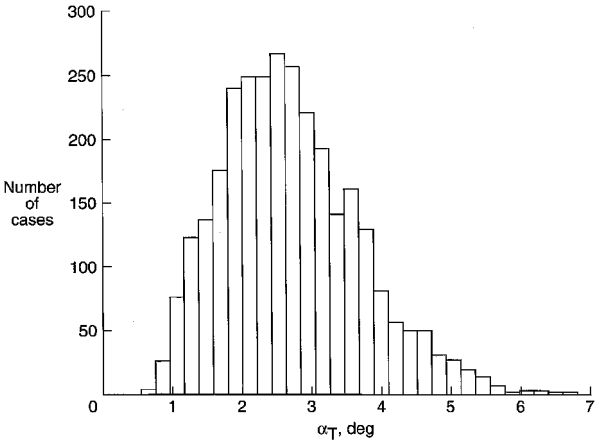

Fig. 9 Distribution of total angle of attack at atmospheric interface resulting from 3000 Monte Carlo simulation cases.

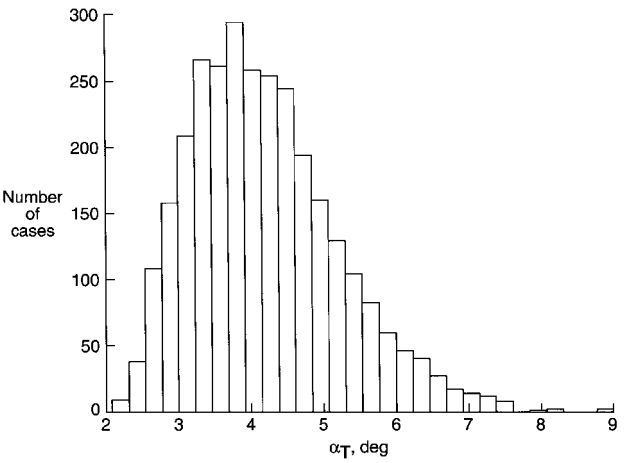

Fig. 10 Distribution of total angle of attack in transitional regime resulting from 3000 Monte Carlo simulation cases.

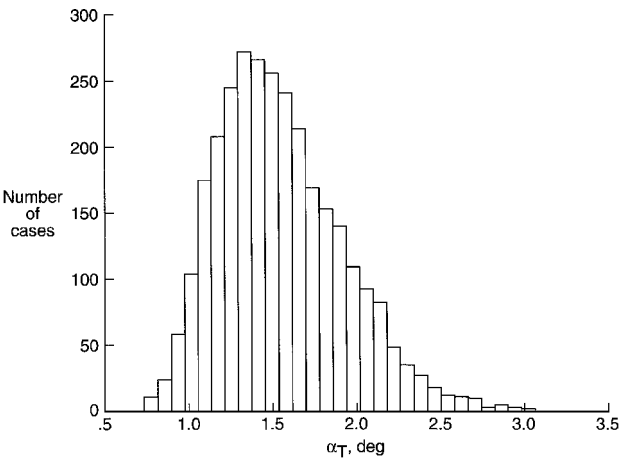

Fig. 11 Distribution of total angle of attack at peak heating resulting from 3000 Monte Carlo simulation cases.

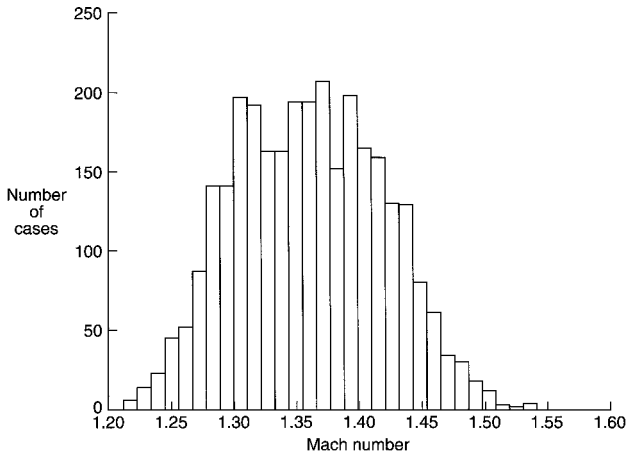

Fig. 12 Distribution of Mach number at drogue chute deployment resulting from 3000 Monte Carlo simulation cases.

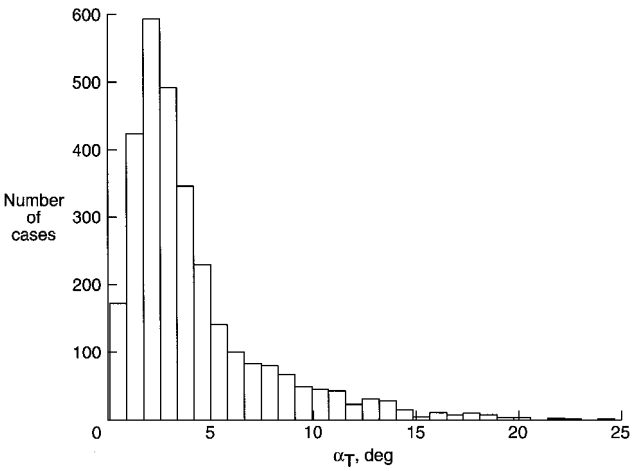

Fig. 13 Distribution of total angle of attack at drogue chute deployment resulting from 3000 Monte Carlo simulation cases.

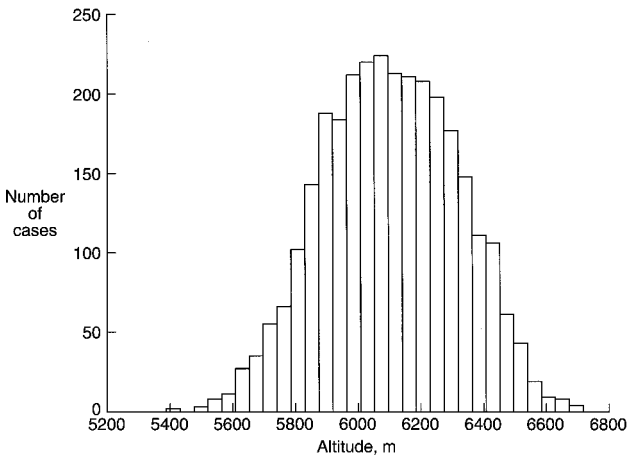

Fig. 14 Distribution of altitude at main chute deployment resulting from 3000 Monte Carlo simulation cases.

angle of attack at three discrete locations during the early phase of the mission: atmospheric interface, transitional regime, and peak heating. At atmospheric interface, the statistical mean total angle of attack of the 3000 Monte Carlo cases is 2.7 deg. The maximum α_T observed is around 6.8 deg (which is below the mission constraint of 10 deg). In the transitional regime (Fig. 10), the total angle of attack does increase (due to the free molecular instability) from atmospheric interface. However, the statistical mean α_T observed is only 4.2 deg, whereas the maximum α_T is 8.9 deg. These values are much lower than the mean and maximum values of 8.5 and 28 deg,

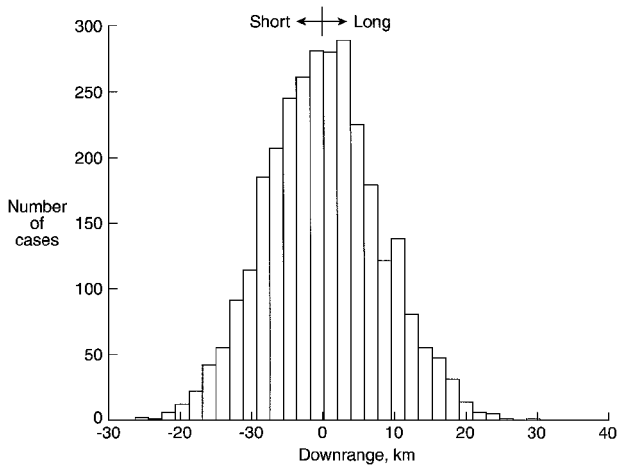

Fig. 15 Downrange distribution of at landing resulting from 3000 Monte Carlo simulation cases.

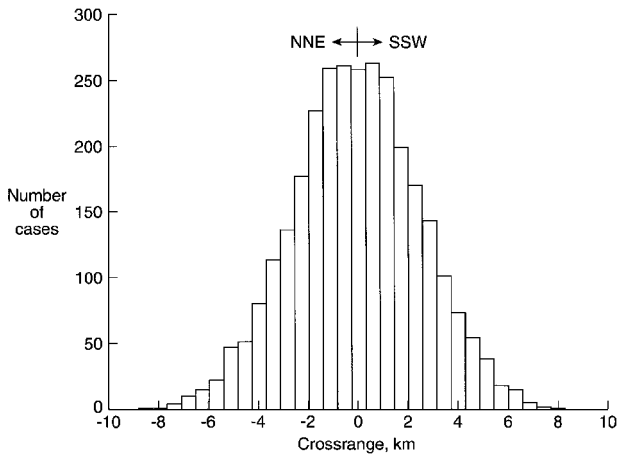

Fig. 16 Crossrange distribution of at landing resulting from 3000 Monte Carlo simulation cases.

respectively, calculated for the Stardust capsule. The higher moments of inertia of the Genesis capsule provide greater gyroscopic stiffness, which retard the effects of the instability. As the SRC descends toward peak heating (where it is stable), the statistical mean α_T decreases to 1.5 deg, as seen in Fig. 11. The maximum α_T observed at peak heating is 3.1 deg (which is well below the mission constraint of 10 deg).

Figures 12–14 show the distribution of the drogue and main parachute deployment conditions. The statistical mean Mach number at drogue chute deployment is 1.36, as seen in Fig. 12. The minimum deployment Mach number encountered is 1.21, which is high enough to avoid the significant effects of the transonic dynamic instability. The corresponding mean total angle of attack at drogue chute deployment (see Fig. 13) is 4.1 deg. The maximum α_T observed is 24.6 deg, which is below the mission constraint of 30 deg. Figure 14 shows the distribution of the main parachute deployment altitude. The statistical mean deployment altitude is 6.1 km, with a minimum occurring at 5.4 km.

The downrange and crossrange distributions at landing for the 3000 Monte Carlo cases are shown in Figs. 15 and 16, respectively. The minimum downrange is −26.3 km (short) from the nominal landing point, whereas the maximum downrange is 30.4 km (long). The maximum crossrange obtained is 8.2 km from the nominal landing point (Fig. 16). The resulting 3-σ ellipse has a major axis of 47.9 km (−23.4 short, 24.5 long) in downrange and a minor axis of 15.2 km in crossrange. A footprint less than 90 km is easily within UTTR. Within the assumptions of the present analysis, a 99.7% probability exists that the SRC will land within this footprint ellipse. Figure 17 shows the landing location of all 3000 Monte Carlo cases. Table 4 summarizes these results. As the capsule design matures and

Table 4 Summary of Monte Carlo analysis

Dispersion	Mean	Minimum	Maximum	3-σ	Mission limit
		Attitude			
Atmospheric interface α_T, deg	2.7	0.5	6.8	2.9	10 deg
Transitional regime α_T, deg	4.2	2.1	8.9	3.1	NA
Peak heating α_T, deg	1.5	0.7	3.1	1.2	10 deg
Drogue chute deployment α_T, deg	4.1	0.1	24.6	10.1	30 deg
		Landing			
Downrange, km	0.1	−26.3	30.4	24.5 (long) −23.4 (short)	<90 km
Crossrange, km	−0.1	−8.8	7.6	7.6	NA
Total range, km	7.0	0.2	30.4	13.6	NA

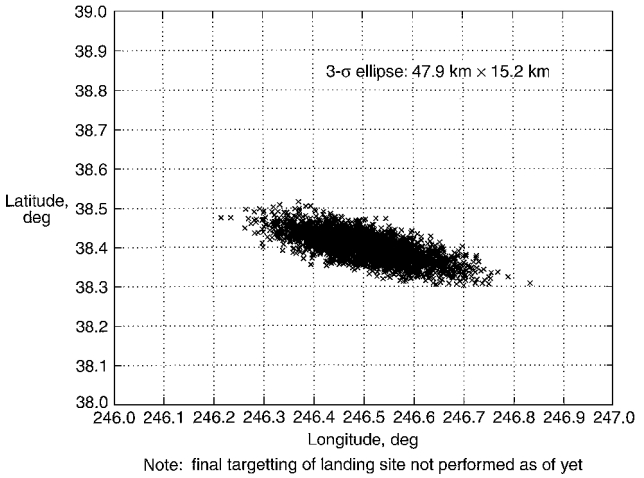

Fig. 17 Landing range dispersion resulting from 3000 Monte Carlo simulation cases.

the aerodynamics characteristics of the SRC are updated, the landing footprint will be refined.

Conclusions

Because of the similarities between the Earth entries of Genesis and Stardust, the Genesis sample return capsule utilizes the entry, descent, and landing sequence developed for Stardust. The nominal entry profile utilizes a gravity switch and two timers for deployment of the drogue and main parachutes. Additionally, due to the similarities of the Genesis and Stardust entry capsules (spherically blunted 60-deg sphere cone forebodies), the Stardust aerodynamic database can serve as the foundation for the Genesis aerodynamics.

Because of the aft c.g. location of the Genesis capsule, aerodynamic instabilities are present during the entry, similar to the Stardust capsule. These instabilities, if not eliminated or at least suppressed, would result in large attitude excursion during the high heating portion of the entry raising concerns of exceeding capsule thermal limits. To suppress these aerodynamic instabilities, gyroscopic stiffness is employed by utilizing a high entry spin rate of 16 rpm.

For the Genesis entry, 47 potential uncertainties were identified that could affect the entry. From a sensitivity analysis, uncertainties in the initial state vector and atmospheric properties (density and north–south and east–west wind components) were found to produce the greatest downrange dispersions on the order of 15–20 km each. A Monte Carlo analysis of 3000 off-nominal trajectories shows that the SRC attitude near peak heating and drogue chute deployment to be within Genesis mission limits. The resulting 3-σ landing footprint obtained was 47.8 km in downrange by 15.2 km in crossrange (which is within the UTTR boundaries). Within the assumptions of the present study, a 99.7% probability exists that the Genesis capsule will land within this ellipse. As the capsule design matures, the landing footprint will be refined.

References

[1]Bell, J. L., Lo, M. W., and Wilson, R. S., "Genesis Trajectory Design," American Astronautical Society, AAS Paper 99-398, Aug. 1999.

[2]Willcockson, W. H., "Stardust Sample Return Capsule Design Experience," *Journal of Spacecraft and Rockets*, Vol. 36, No. 3, 1999, pp. 470–474.

[3]Desai, P. N., Mitcheltree, R. A., and Cheatwood, F. M., "Entry Dispersion Analysis for the Stardust Comet Sample Return Capsule," *Journal of Spacecraft and Rockets*, Vol. 36, No. 3, 1999, pp. 463–469.

[4]Desai, P. N., Mitcheltree, R. A., and Cheatwood, F. M., "Entry Trajectory Issues for the Stardust Sample Return Capsule," International Symposium on Atmospheric Reentry Vehicles and Systems, Paper 15.1, Association Aeronautique et Astronautique de France, March 1999.

[5]Mitcheltree, R. A., Wilmoth, R. G., Cheatwood, F. M., Brauckmann, G. J., and Greene, F. A., "Aerodynamics of Stardust Sample Return Capsule," *Journal of Spacecraft and Rockets*, Vol. 36, No. 3, 1999, pp. 429–435.

[6]Cheatwood, F. M., and Gnoffo, P. A., "User's Manual for the Langley Aerothermodynamic Upwind Relaxation Algorithm (LAURA)," NASA TM 4674, April 1996.

[7]Mitcheltree, R. A., and Fremaux, C. M., "Subsonic Dynamics of Stardust Sample Return Capsule," NASA TM 110329, March 1997.

[8]Brauer, G. L., Cornick, D. E., and Stevenson, R., "Capabilities and Applications of the Program to Optimize Simulated Trajectories (POST)," NASA CR-2770, Feb. 1977.

[9]Braun, R. D., Mitcheltree, R. A., and Cheatwood, F. M., "Mars Microprobe Entry-to-Impact Analysis," *Journal of Spacecraft and Rockets*, Vol. 36, No. 3, 1999, pp. 412–420.

[10]Braun, R. D., Powell, R. W., Engelund, W. C., Gnoffo, P. A., Weilmuenster, K. J., and Mitcheltree, R. A., "Mars Pathfinder Mission Six-Degree-of-Freedom Entry Analysis," *Journal of Spacecraft and Rockets*, Vol. 32, No. 6, 1995, pp. 993–1000.

[11]Desai, P. N., Braun, R. D., Powell, R. W., Engelund, W. C., and Tartabini, P. V., "Six-Degree-of-Freedom Entry Dispersion Analysis for the METEOR Recovery Module," *Journal of Spacecraft and Rockets*, Vol. 34, No. 3, 1997, pp. 334–340.

[12]Justus, C. G., Jeffries, W. R., III, Yung, S. P., and Johnson, D. L., "The NASA/MSFC Global Reference Atmospheric Model—1995 Version (GRAM-95)," NASA TM-4715, Aug. 1995.

[13]Spencer, D. A., Blanchard, R. C., Braun, R. D., Kallemeyn, P. H., and Thurman, S. W., "Mars Pathfinder Entry, Descent, and Landing Reconstruction," *Journal of Spacecraft and Rockets*, Vol. 36, No. 3, 1999, pp. 357–366.

[14]Mitcheltree, R. A., Fremaux, C. M., and Yates, L. A., "Subsonic Static and Dynamic Aerodynamics of Blunt Entry Vehicles," AIAA Paper 99-1020, Jan. 1999.

C. A. Kluever
Associate Editor